



VCU

Virginia Commonwealth University
VCU Scholars Compass

Theses and Dissertations


Graduate School

2023

Contribution of Metabolic Cell Swelling on Microcirculatory Perfusion in Septic Shock

Charles E. Payne
Virginia Commonwealth University

Follow this and additional works at: <https://scholarscompass.vcu.edu/etd>

 Part of the [Circulatory and Respiratory Physiology Commons](#), [Critical Care Commons](#), [Medical Biophysics Commons](#), [Medical Immunology Commons](#), [Medical Physiology Commons](#), and the [Physiological Processes Commons](#)

© Charles Payne

Downloaded from

<https://scholarscompass.vcu.edu/etd/7235>

This Thesis is brought to you for free and open access by the Graduate School at VCU Scholars Compass. It has been accepted for inclusion in Theses and Dissertations by an authorized administrator of VCU Scholars Compass. For more information, please contact libcompass@vcu.edu.

Contribution of Metabolic Cell Swelling on Microcirculatory Perfusion in Septic Shock

Virginia Commonwealth University
Graduate School

© Charles Payne _____ 2023
All Rights Reserved

Contribution of Metabolic Cell Swelling on Microcirculatory Perfusion in Septic Shock

A thesis submitted in partial fulfillment of the requirements for the degree of
Master of Science at Virginia Commonwealth University

by

Charles Ercil Payne
B.S. from Virginia Commonwealth University, 2021

Director: Martin Mangino, PhD
Department of Surgery
Department of Physiology and Biophysics

Virginia Commonwealth University
Richmond, Virginia
April, 2023

Table of Contents

| | |
|--|----|
| ACKNOWLEDGEMENTS | iv |
| LIST OF FIGURES, TABLES, AND EQUATIONS | v |
| LIST OF ABBREVIATIONS | vi |
| ABSTRACT | 1 |
| INTRODUCTION | 3 |
| <i>Sepsis and Septic Shock</i> | 3 |
| <i>Clinical Relevance</i> | 3 |
| <i>Microcirculation and Physiology of Oxygen Transport</i> | 4 |
| <i>Effects of Septic Shock on Intestinal Mucosa and Microcirculation</i> | 6 |
| <i>Metabolic Cell and Tissue Swelling</i> | 7 |
| <i>Cell Impermeants</i> | 8 |
| <i>Polyethylene Glycol 20,000</i> | 9 |
| <i>Glycocalyx and Syndecan-1</i> | 9 |
| <i>Purpose of Study</i> | 10 |
| MATERIALS AND METHODS | 12 |
| <i>Lipopolysaccharide Infusion</i> | 12 |
| <i>Cecal Ligation and Puncture</i> | 14 |
| <i>Vital Sign Monitoring</i> | 16 |
| <i>Arterial Blood Gas and Venous Samples</i> | 16 |
| <i>Lipopolysaccharide</i> | 17 |
| <i>PEG-20K and Lactated Ringers</i> | 17 |
| <i>Orthogonal Polarization Spectral Imaging</i> | 18 |
| <i>Syndecan-1 ELISA</i> | 20 |
| <i>Statistical Analysis</i> | 20 |
| <i>Troubleshooting</i> | 21 |
| RESULTS | 22 |
| <i>OPSI Analysis</i> | 22 |
| <i>Lab Values</i> | 25 |
| <i>Vital Signs and Survival Time</i> | 29 |
| <i>Syndecan-1 Assay</i> | 31 |

| | |
|--|----|
| DISCUSSION | 32 |
| <i>Major Findings</i> | 32 |
| <i>Microcirculatory Changes</i> | 33 |
| <i>Lactate, Survival Time, and Vital Signs</i> | 35 |
| <i>Presence of Sydecin-1</i> | 38 |
| <i>Limitations and Future Studies</i> | 38 |
| CONCLUSION | 41 |
| REFERENCES | 43 |
| APPENDICES | 46 |
| VITA | 49 |

ACKNOWLEDGEMENTS

Thank you, Dr. Mangino for believing in me and challenging me to do more and be more than I ever thought I could be. To Dr. Pittman, an incredible wealth of knowledge, advice, and guidance from our very first meeting. To Dr. Leichtle, a professional role model and mentor that I have looked up to for years. To Dr. Bradley, for her unending cheer and eager assistance. To Nancy, from help with experiments to a friendship I will forever cherish. To Christina, who has always built me up and given me every tool I needed to be successful. To Dr. Liebrecht, who has only ever wanted to see me succeed.

Thank you, to my now wife Tiana, who has been a constant source of unconditional support and love that is the heart of all my successes. To my mother, who has believed in me since day one. To Chunk, who knew and spread only happiness even on the darkest days. To Dan and Joey, dear friends and true champions of my well-being, who always ensured I approached every situation with care, thoughtfulness, and compassion. And to all those friends, family, acquaintances, and strangers who have helped me along in their own way: thank you.

This work was funded by NIH R41GM143995, Department of Defense W81XWH-18-10759, and W81XWH-16-2-0040

LIST OF FIGURES, TABLES, AND EQUATIONS

| | |
|---|--------|
| Figure 1. Mechanism of Action of PEG-20K | 9 |
| Figure 2. LPS Experimental Design | 13 |
| Figure 3. CLP Experimental Design | 15 |
| Figure 4. Still Photo of an OPSI Video | 19 |
| Figure 5. Average LPS Rat MFI and PPV% Graphs | 22 |
| Figure 6. Average CLP Rat MFI and PPV% Graphs | 24, 25 |
| Figure 7. LPS Lactate Graph | 26 |
| Figure 8. LPS Glucose Graph | 27 |
| Figure 9. CLP Lactate Graph | 28 |
| Figure 10. CLP Glucose Graph | 28 |
| Figure 11. LPS MAP and HR Graphs | 29 |
| Figure 12. CLP MAP and HR Graphs | 30 |
| Figure 13. LPS PEG vs. LR Survival | 30 |
| Figure 14. LPS Syndecan-1 | 31 |
| | |
| Table 1. Blinded Analysis | 23 |
| Table 2. Baseline LPS | 26 |
| Table 3. Shock LPS | 26 |
| Table 4. CLP Shock | 28 |
| | |
| Equation 1. Poiseuille's Law | 5 |

LIST OF ABBREVIATIONS

ABG – Arterial Blood Gas

BPM – Beats per Minute

CBC – Complete Blood Count

CLP – Cecal Ligation Puncture

Hb – Hemoglobin

HR – Heart Rate

LPS – Lipopolysaccharide

LR – Lactated Ringers

LVR – Low Volume Resuscitation

MAP – Mean Arterial Blood Pressure

MFI – Microvascular Flow Index

OPSI – Orthogonal Polarization Spectral Imaging

PEG-20K – Polyethylene Glycol 20,000

PPV% - Proportion of Perfused Small Vessels

ABSTRACT

Sepsis is a medical emergency that nearly six million people die from annually worldwide. A systemic immunological response that leads to organ-dysfunction, the development of septic shock, and death has mortality rate of 15-25%. The far more lethal subset of sepsis, septic shock, has an in-hospital mortality rate of 30-50%. In addition to the significantly high mortality rate, sepsis and its treatment is the most expensive healthcare problem in the United States with the US Agency for Healthcare Research and Quality estimating annual costs over \$20 billion. ¹ Significant progress has been made in the area of understanding and refining the definition, early recognition, and supportive treatments for sepsis, however, treatments that make meaningful interventions in the outcomes are lacking. During the progression of sepsis into septic shock multiple body systems become poorly perfused and hypoxic as a result of the complex and interweaving inflammatory responses. This hypoxia induces metabolic cell and tissue swelling that leads to further microcirculatory dysfunction and poor tissue perfusion. Conversely, reversing metabolic cell swelling corrects these perfusion defects. This is my project hypothesis. To determine the role septic shock plays in microcirculation and perfusion, two models were used in rats to induce septic shock. The lipopolysaccharide (LPS) model relied on an infusion of LPS to induce an acute systemic inflammatory response; the second model of cecal ligation and puncture (CLP) involved puncturing the cecum of a rat with a needle to create holes for stool to slowly leak into the abdomen and induce a polymicrobial peritoneal sepsis over the course of two days. Both models put the rats into a state of septic shock, and both caused significant (over 50%) reduction in microcirculatory perfusion in the ileum. Polyethylene glycol 20,000 (PEG-20K), an inert cell

impermeant that moves metabolic cell water out of the cell into capillaries to improve perfusion in shock,² was used as a research tool to test the hypothesis. PEG-20K and lactated Ringer's (LR) solutions were used as low volume resuscitation (LVR) treatments for comparison. The microcirculation of the terminal ileum was monitored at baseline, shock, and at different time point's post-LVR using Orthogonal Polarization Spectral Imaging (OPSI) to record and analyze the quality of perfusion. Vital signs of mean arterial blood pressure (MAP), heart rate, and temperature were monitored throughout and 75% of baseline MAP was used to indicate septic shock. A MAP at 75% of baseline has been a point in which our lab has gotten consistent data that shows physiological changes. Arterial and venous blood samples were taken to measure arterial blood gas laboratory values and serum. Septic shock was successfully induced in both models and on OPSI observation showed a significant decrease in microcirculatory perfusion compared to baseline. PEG-20k caused a significant improvement in perfusion after treatment, improved survival outcomes, reduced the need for vasopressors, and improved secondary cardiovascular outcomes, relative to the LR controls. Our findings indicate that septic shock induced a severe decrease in microcirculatory perfusion in the bowel and that PEG-20K can serve as an efficient tool to help correct these microcirculatory deficiencies. Reversal of perfusion defects with osmotic impermeants like PEG-20k in septic shock suggests the mechanism is due, in part, to water shifts into the cell and tissue that cause compression no-reflow.

INTRODUCTION

Sepsis and Septic Shock

Sepsis has been, at the very least, recognized as early as 1,000 BC; sepsis and how to treat it has boggled the minds of scientists and clinicians alike for nearly 3,000 years.³ Over time its definition has evolved from putrefaction of blood and tissues with fever³ to its 1991 definition ‘systemic inflammatory response to a microbial infection’⁴ to the modern day definition in 2015 – Sepsis is a clinical condition of life-threatening organ dysfunction that is caused by an uncontrolled and dysregulated response to infection.⁵ Septic shock is a subset of sepsis in which underlying circulatory and cellular metabolism abnormalities are significant enough to substantially increase mortality.

While mortality rates of sepsis have been slowly declining, they still sit in the 15-25% range and a significant spike in mortality is seen when sepsis progresses to septic shock with in-hospital mortality rates anywhere from 30% to as high as 50%.¹ The pathogenesis of sepsis is an incredibly complex process with several interweaving factors beyond the realm of inflammation and microbial or host pattern recognition. Primary and secondary immune tissues, coagulation, parenchymal tissues, and changes in endothelial tissues and microcirculation all have a role to play in the progression of sepsis into septic shock.

Clinical Relevance

The treatment of sepsis is the most expensive condition treated in hospitals in the United States, per the US Agency for Healthcare Research and Quality, and has annual costs that exceed \$20 billion.¹ In addition to this, the US Centers for Medicare and Medicaid Services has put significant financial penalties in place for hospitals and institutions that fail to appropriately

recognize and treat sepsis early. Even though significant improvements have been made in the understanding of sepsis, its recognition, and progression, our ability to intervene and change the course of the disease remains limited. In other words, the knowledge gained is disproportionate to the improved outcomes seen. Despite in-hospital mortality rates decreasing over the years, these improvements can generally be attributed to earlier recognition and early implementation of supportive therapies.⁶ It is the combination of early recognition and diagnosis with improved treatments that address root problems like poor microcirculation and perfusion that will truly improve patient outcomes.

Microcirculation and Physiology of Oxygen Transport

The microcirculation consists of microvessels with diameters $<100\ \mu\text{m}$ that make up the terminal vascular network of the systemic circulation. Microvessels within this network are arterioles, post-capillary venules, capillaries, and their respective cellular constituents. It serves as the last stop of the cardiovascular system that in general is responsible for the transfer of oxygen from red blood cells (RBC) in the capillaries to parenchymal cells where the oxygen is delivered. The delivery of oxygen serves to meet and maintain energy requirements of the tissue cells and support their vital functional activities. In addition to this vital function, the microcirculation is also responsible for the regulation of solute exchange between the intravascular and tissular space and the transport of hormones and nutrients to the tissue cells and maintaining functional homeostasis. The microcirculation also delivers antibiotics and other therapeutic molecules to infected tissues.

Oxygen transport is achieved by two means within the capillaries, the convection of oxygen-carrying RBCs and diffusion of oxygen from RBCs to the mitochondria in the tissue

cells.⁷ Convection is the movement of oxygen within the circulation and occurs through bulk transport. This process is active and requires energy that is derived from the pumping of the heart. Diffusion is the passive movement of oxygen down its concentration gradient, from the microcirculation to the tissues and finally the mitochondria.⁸ Oxygen flux may be altered through changes in cardiac output and oxygen content, however, at the level of the microvessels, factors like diffusion distance and vessel diameter have an enormous impact on oxygen flux. Both factors can be negatively influenced in the presence of a critical illness such as sepsis or septic shock.

The French physicist and physiologist Jean Léonard Marie Poiseuille experimentally derived, formulated, and published Poiseuille's law for laminar flow, which uses an equation (Equation 1) to describe laminar flow through a tube, or the flow of blood through capillaries. This equation shows the incredible impact that the diameter of the vessels (r^4) has on the flow (Q) through the vessel, where radius (r) influences the flow (Q) to the power of four.⁹ In other words, just small changes in compressible vessel radius caused by local cell and tissue swelling can have an enormous impact on flow through the vessel and consequently, the oxygen flux and perfusion of surrounding tissue.

$$Q = \frac{\Delta P \pi r^4}{8 \eta l}$$

Equation 1. Poiseuille's Law – Poiseuille's law for flow where Q = volume flow, ΔP = change in pressure, r = vessel radius, η = viscosity, and l = vessel length

The amount of substance or oxygen that can be exchanged can be increased by opening more capillaries. When more capillaries are opened, the surface area for exchange is increased and the diffusion distance is reduced, thereby increasing the overall efficiency of diffusion. This

capillary recruitment to meet metabolic demands was demonstrated by August Krogh in 1919.¹⁰ Just as opening more capillaries makes diffusion more efficient, the closing off of capillaries as in critical illness increases diffusion distance and decreases diffusion efficiency. In this experiment the effects of critical illness in the form of septic shock on the microcirculation will be examined and measured for analysis to test our metabolic swelling hypothesis.

Effects of Septic Shock on Intestinal Mucosa and Microcirculation

Although sepsis is defined by life-threatening systemic organic dysfunction in critically ill patients, the local alterations and their consequences to individual body systems like the intestinal mucosal system cannot be overlooked. The small intestinal mucosa contains a monolayer of simple columnar epithelium, consisting primarily of absorptive cells and scattered goblet cells with occasional enteroendocrine cells. This layer serves to transport nutrients and also proved a barrier between the lumen and the body compartments. The endothelium can recruit inflammatory cells and generate an overwhelming pro-inflammatory response to pathogen-associated molecular patterns (PAMPs) like the lipopolysaccharide (LPS) used in our rat model.^{11,12} Upon being recruited to the intestinal tissue, neutrophils and macrophages produce pro-inflammatory cytokines and begin local and systemic inflammation.¹³ Alterations to the gut barrier homeostasis in this way can alter mucus layer formation and composition, increase the permeability of epithelial cells, and further damage these cells with subsequent inflammatory signaling.¹³ The endothelial dysfunction and disturbances in gut vasculature and perfusion in sepsis made the terminal ileum the perfect candidate to observe microcirculatory changes throughout both experiments in this study. In addition to the gut microcirculation being accessible to study, it may also serve as an end organ whose failure from ischemia in sepsis or

primary trauma causes further septic shock by promoting bacterial and enterotoxin translocation across the septic barrier in a self-amplifying cycle.

Gut barrier dysfunction begins a cascade that can be the result of sepsis, leading to increased permeability, dysfunctional mucosal perfusion, tissue edema, and coagulation dysregulation. In the setting of septic shock, entire systems begin to become hypoperfused and hypoperfusion in the splanchnic region is one of the primary reasons for mucosal gut barrier breakdown. The splanchnic vascular system that generally receives about 25% of the total cardiac output becomes a cytokine-generating organ during hypoperfusion, generating cytokines^{13,14} that lead to further dysfunction through the circulation. These cytokines target blood cells, endothelium, and vascular smooth muscle and lead to vasodilation, capillary leakage, increased venous capacity and decreased venous return. All these effects lead to an eventual decline in cardiac output and tissue perfusion.¹⁵

Metabolic Cell and Tissue Swelling

Metabolic cell and tissue swelling is a consequence of ischemia induced by circulatory shock and appears to be a root cause that leads to malperfusion in tissues and organs and eventually death.^{2,16,17} When parenchymal and stromal cells within the microcirculation become hypoxic, they lose the ability to perform aerobic ATP synthesis. Once ATP becomes limited or is exhausted completely, the sodium-potassium ATPase is no longer able to function appropriately. This pump is a crucial transmembrane ATPase that is found in the membranes of all animal cells and its status as an active pump relies on the availability of ATP to perform its job of exporting three sodium ions and importing two potassium ions. Once this pump stops functioning, sodium begins to enter the cell, moving with its electrochemical gradient, with chloride following it. As

sodium chloride levels rise, water follows into cells down the osmotic gradient created by the sodium pump failure, leading to cell and tissue swelling. This cell and tissue swelling causes microcirculatory compression and what we term “compression no-reflow,” thus further exacerbating ischemia as perfusion and oxygen delivery are retarded, even when blood and fluids are administered during resuscitation. Reversal of this metabolic cell and tissue swelling restores flow and oxygenation throughout the microcirculation in hemorrhagic shock. We hypothesize that a similar mechanism can cause poor tissue perfusion in septic shock.

Cell Impermeants

Impermeants are inert molecules that are impermeant to cells, but can leave the capillaries. Generally, these molecules are saccharides and small organic cations and anions, which are small enough to freely leave the capillary space while at the same time being too large or too charged to cross the cell membrane. These cells can preferentially load into the interstitial space and create an osmotic force to pull water out of cells and prevent further water from entering cells during ischemia-induced osmotic shifts. Today cell impermeants make up a critical component of organ preservation solutions with raffinose, lactobionic acid, gluconate, sulfate, and phosphate all being recognized as cell impermeants. These compounds are found in high concentrations in University of Wisconsin solution, the gold standard solution used in organ preservation and transplant.² Colloids, such as albumin and fresh frozen plasma, are similar in that they can set-up similar osmotic gradients and are impermeant to cells; however, they differ in that they do not leave the capillary space.

Polyethylene Glycol 20,000

Polyethylene Glycol 20,000 (PEG-20K) IV solution is an impermeant-based resuscitant that was created in the Mangino laboratory at Virginia Commonwealth University as a tool to help mitigate metabolic cell and tissue swelling. PEG-20K is an impermeant with an osmotic reflection coefficient (σ_d) of about 0.5, meaning that for every two molecules that stay in the capillary space, one exits and enters the interstitial space and two stay in the capillary space. Therefore, PEG-20K has been termed a cell impermeant and colloid hybrid.¹⁶ This means that two gradients for water transfer are formed and a non-energetic transfer of water out the cell and into the capillary occurs (Figure 1). In addition to these two gradients, PEG-20K also benefits from an incredibly hydrophilic oxo-ether backbone that helps to attract water. This tool has been shown to work significantly better than simple impermeants like gluconate anions.^{16,17} A 10% solution of PEG-20K in LR was used as a treatment group in the experiments throughout this study.

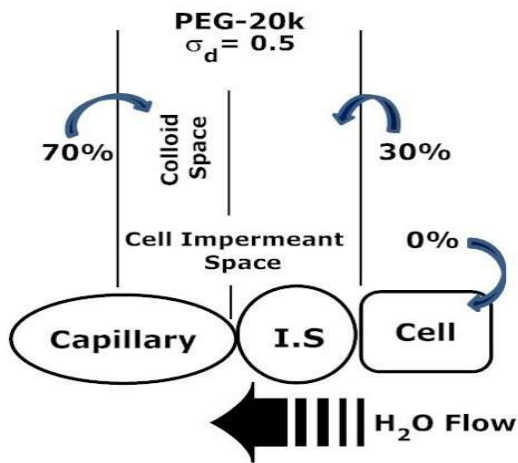


Figure 1 Mechanism of action of PEG-20K

- The osmotic reflection coefficient (σ_d) of PEG-20K molecules is about 0.5, meaning that for every two molecules of PEG-20K that is within the capillary space, one is within the interstitial space. This creates two osmotic gradients that work through a non-energetic transfer of isotonic water out of the cells and interstitial space and into the capillary.¹⁶

Glycocalyx and Syndecan-1

All along the luminal surface of vascular endothelial cells of the small bowel is a gel-like layer made up of membrane-attached proteoglycans, glycosaminoglycan chains, glycoproteins,

and adherent plasma proteins. This layer is known as the endothelial glycocalyx and it helps to maintain homeostasis of the vasculature by controlling its permeability and microvascular tone and regulating leukocyte adhesion.¹⁸ During sepsis and septic shock this layer can be degraded through inflammatory mechanisms like metalloproteinases, heparanase, and hyaluronidase, all commonly referred to as sheddases. Septic shock-induced reactive oxygen species and pro-inflammatory cytokines, like tumor necrosis factor alpha (TNF- α) and interleukin-1beta (IL1B), activate these sheddases.

Proteoglycans are the core proteins that are anchored to the apical membrane of endothelial cells and one of them, Syndecan-1, and its presence in the degradation of the glycocalyx has been a common area of study.¹⁹ Syndecan-1 appears to be the most common type in the luminal surface of epithelial cells and so is an excellent marker to indicate the degradation of the glycocalyx during septic shock as it is shed from the microcirculation and ends up in the plasma.²⁰ In this study, Syndecan-1 was used as a marker for glycocalyx degradation measured in baseline and terminal serum samples. We tried to test an alternative hypothesis to explain effects observed with the polymers used in this study. Specifically, we tested whether nonspecific adherence of PEG-20k to the endothelium could improve outcomes and perfusion in these studies by protecting the glycocalyx from degradation or acting as an artificial surrogate glycocalyx barrier after it degrades.

Purpose of Study

The purpose of this study was to test whether metabolic tissue and cell swelling contributes to perfusion defects caused by septic shock. Previous studies in the lab have shown PEG-20K to be an incredibly effective tool in improving survival outcomes in hypovolemic shock models by leveraging this mechanism.¹⁷ To understanding of the effectiveness of PEG-

20K and the role that critical illness, in the form of septic shock, plays on the microcirculation and perfusion, this study sought to induce septic shock using two different models and then use PEG-20K as a tool to improve the microcirculation and perfusion. The aim of the study was to determine whether metabolic cell and tissue swelling contributes to perfusion defects in septic shock and to downstream multiple organ failure.

The study replicated septic shock using an infusion of lipopolysaccharide to induce a systemic inflammation response and elicit hemodynamic instability and decreased microcirculatory perfusion. Additionally, a second model of polymicrobial peritoneal sepsis, a form of sepsis more likely to be seen in an intensive care unit, was also used. Both models used Orthogonal Polarization Spectral Imaging to analyze the microcirculation of the bowel at the terminal ileum throughout each experiment and during treatment with PEG-20K or lactated Ringer's solution.

MATERIALS AND METHODS

Lipopolysaccharide Infusion

Male Sprague-Dawley rats were anesthetized with 4% isoflurane and oxygen for 4 minutes and reduced to 2% isoflurane and oxygen for a remainder of the procedure, with minor adjustments made as needed. The rat was then weighed, and bilateral femoral regions, abdomen, and neck were shaved, cleaned, and prepped with a chlorohexidine solution. The rat was placed on a heating pad for the remainder of the procedure with a rectal temperature probe inserted for constant monitoring through the LabCharts software. Bilateral femoral arterial and venous lines were placed with an initial cut to break the skin followed by blunt dissection down to and for cleaning the vessels (Figure 2). The artery and vein were cannulated with polyethylene-50 and polyethylene-90 tubing, respectively. An arterial line was connected to a pressure transducer captured by a data acquisition system (PowerLab) for constant vital sign monitoring. An incision was then made to open the abdomen and locate the cecum, tracing from the cecum to find the terminal ileum. An enterotomy was performed on the terminal ileum and it was cleaned of mucus and feces using a syringe filled with warm lactated Ringer's solution and soft blotting with gauze to ensure the integrity of the fragile bowel. Baseline OPSI videos as well as 0.25 mL of arterial and 1.0 mL of venous blood were collected. After OPSI was obtained throughout the experiment the bowel was carefully placed back in the abdomen, with the abdomen being closed temporarily using a Backhaus towel clamp and being covered by moist gauze. The first LPS infusion was given at 5-15 mg/kg in 1 mL of LR given at 0.1mL/min using the venous line; the dose of LPS varied based on the variable efficacy of LPS batches. During this infusion and for a few minutes afterwards, the rat's MAP dropped close to shock range of 75% of baseline and quickly

recovered to baseline where the second dose of LPS was started using the same amount of LPS as the first dose except given at a rate of 0.01mL/min.

A second dose was given until shock was reached, defined as a MAP that was 75% of the baseline. Just prior to reaching the critical 75% range, generally around the 80-85% range, OPSI was taken, and arterial blood gas samples were obtained. Shortly after samples were taken, the rat would be in the 75% MAP range and the LPS infusion was stopped and LVR started with either LR or PEG-20K in LR, each dosed at a volume of 6.8 mL/kg given over 5 minutes. OPSI data and arterial blood samples were taken 30 and 60 minutes after shock with further samples being taken hourly. When the rat had a MAP that was no longer appropriate to sustain life (<35 mmHg), terminal venous samples for serum were taken and the rat was euthanized via thoracotomy and anesthesia overdose. Immediately after euthanasia, samples of bowel, kidney, liver, lung, and heart were collected and placed in formalin.

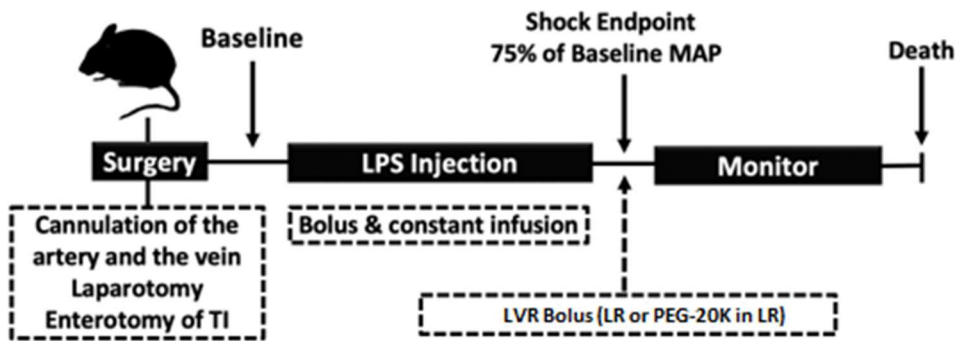


Figure 2 LPS Experimental Design – Sprague-Dawley rats were anesthetized, their femoral vein and arteries cannulated, abdomen opened, and enterotomy performed on terminal ileum. After baseline labs and OPSI samples were taken they were given an IV bolus of lipopolysaccharide (LPS) followed by a slower constant infusion of a more dilute LPS solution until shock was reached, indicated by 75% of baseline MAP. The LPS infusion was then discontinued, and a low volume resuscitation was given, either LR or PEG-20K in LR, and rat was monitored until MAP reached 35.

Cecal Ligation and Puncture

The cecal ligation and puncture model took place over two days with two separate surgical procedures. On the first day, male Sprague-Dawley rats were anesthetized with 4% isoflurane and oxygen for 4 minutes and reduced to 2% isoflurane and oxygen for the remainder of the procedure, with minor adjustments made as needed. The rat was then weighed, and bilateral femoral regions, abdomen, and neck were shaved, cleaned, and prepped with a chlorohexidine solution. The rat was placed on a heating pad for the remainder of the procedure with a rectal temperature probe inserted for constant monitoring through the LabCharts program. Using sterile technique, a single femoral arterial and venous line was placed with an initial cut to break the skin followed by blunt dissection down to and for cleaning the vessels. The artery and vein were cannulated with polyethylene-50 and polyethylene-90 tubing, respectively. The arterial line was hooked up to an arterial line transducer connected to a computer for continuous vital sign monitoring as well as baseline lab values; VBG, CBC, and CMP were obtained. The abdomen was then opened along the midline with a 3-4 cm incision. The cecum was located and gently mobilized outside of the abdomen and the ileo-cecal junction was visualized. Using 2-0 silk 50% of the cecum was ligated and 4 through-and-through holes were made in the cecum distal to the tie using an 18-gauge needle (Figure 3). The cecum was gently placed back into the abdomen and the abdomen was closed in two layers using a running 2-0 proline for the peritoneum and muscle layer and 4-0 silk for the skin. The vascular cannulae were removed, the vessels ligated, and the wounds were closed with 4-0 silk. A weight-based dose of Buprenorphine SR was given at the nape and the rat was recovered from surgery in a cage with a

heating pad under half of it to ensure the rat would not overheat if it got too warm for comfort. The rat was monitored every 12 hours for wellness, general appearance, and suture check.

At the 24-hour mark the rat we anesthetized again using 4% isoflurane and oxygen for four minutes and brought down to 2% isoflurane and oxygen for the remainder of the procedure. Arterial and venous catheters were placed in the femoral artery and vein in the same fashion as day one and the arterial line hooked up to LabCharts for vital sign monitoring. The terminal ileum was located and gently removed from the abdomen followed by an enterotomy and cleaning of mucus and feces from the OPSI site prior to taking pre-treatment OPSI samples followed by pretreatment ABG and venous samples. The rat was then given LVR with either LR or 10% PEG-20K in LR (6.8 ml/kg) over five minutes with OPSI taken at the 30- and 60-minute post-LVR time-points as well as ABGs. Animals were euthanized using anesthesia overdose and thoracotomy when MAP was no longer suitable to sustain life at 35 mmHg.

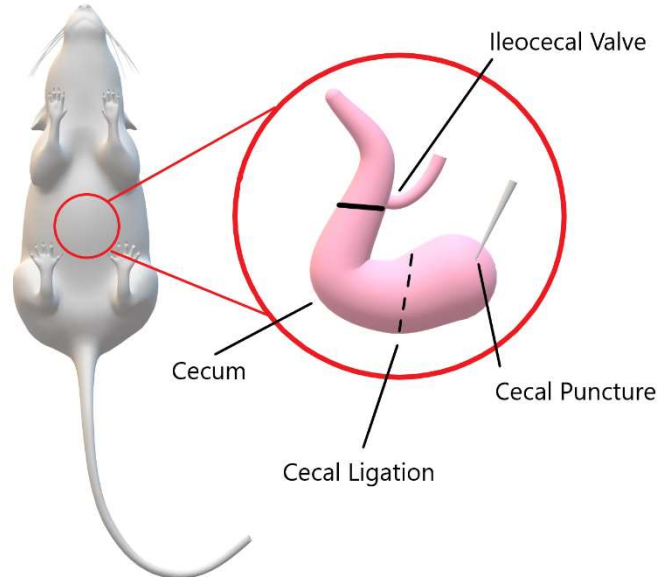


Figure 3 CLP Experimental Design - Cecal ligation and puncture experimental design. After a midline laparotomy, cecum was gently removed from the abdomen and ileocecal valve identified. Cecum was ligated at the midpoint between valve and end of the cecum (50%) and punctured with an 18g needle 4 times through-and-through. Cecum placed back in abdomen and abdomen closed.

Vital Sign Monitoring

Vital signs including mean arterial blood pressure (MAP - mmHg), heart rate (HR - BPM), and temperature were monitored throughout each experiment using a femoral arterial line hooked up to an arterial transducer that was connected to an ADInstruments Bio Amp. This Bio Amp worked in conjunction with the PowerLab data acquisition system and LabChart analysis software to allow for continuous monitoring and recording of real time MAP, HR, and temperature. The rectal temperature probe was also monitored through the same program and amp. Respiratory rate was recorded by counting manually at specific time intervals.

Arterial Blood Gas and Venous Samples

For both models, arterial blood gas and venous samples were collected from the femoral artery and vein, respectively. When femoral venous access was difficult, the jugular vein was accessed in its place; blood draws and infusions were given in the same fashion as with the femoral vein. For an arterial blood gas sample, 0.25 mL of arterial blood was drawn at baseline, shock prior to LVR, and every 30 minutes after shock in both models. An ABL800 Flex blood gas analyzer was used and provided the lactate and glucose measurements. For venous blood, 1.00 mL was drawn at baseline and just prior to sacrificing the animal in both experiments. The blood was used for serum samples and CBC labs.

Lipopolysaccharide

Lipopolysaccharides (LPS) are an important component of the cell wall of Gram-negative bacteria. When given to rats, it causes the release of pro-inflammatory mediators like tumor necrosis factor alpha (TNF- α) that begin a systemic inflammatory cascade that leads to systemic inflammation, multiple organ failure, shock, and eventually death. LPS was ordered through Sigma Aldrich where it was extracted from *Escherichia coli* serotype O111:B4 using phenol extraction. To prepare the powdered LPS for infusion the two batches were dissolved in 1mL and 3 mL of LR at a dose of 5-15mg/kg depending on the potency of the specific batch used. During the experiment it was given at two points, the first more concentrated dose was given over 10 minutes (0.1 mL/min) after baseline vitals, labs, and OPSI samples were taken. This first infusion would generally drop the MAP to shock range (~75% of the baseline MAP) and recover within 15 minutes of the infusion ending, acting to precondition the animal to going into septic shock more gracefully and within a reasonable amount of time during the second infusion. The second dose was given at a slower rate of 0.01mL/min after the first infusion was completed and the animals MAP returned to baseline, generally about 15 minutes after the completion of the first dose. This second dose was given until the animal reached septic shock which was defined as a MAP at 75% of their baseline. Once this point was reached and the dose was stopped LVR was started immediately.

PEG-20K and Lactated Ringers

Polyethylene glycol 20,000 (PEG-20K) and lactated Ringer's (LR) solution were used for low volume resuscitation (LVR) in both the LPS and CLP models. Sterile bags of LR were used

for all infusions and line flushing as needed, pulling needed fluid from bags with sterile technique. LR that was used for washing of the bowel was first transferred to a specimen cup and then placed and kept in a warm water bath throughout the experiments, pulling fluid from the specimen cup as needed. PEG-20K was ordered in a powder form from Sigma Aldrich and 500 mL batches of 10% PEG-20K in LR were made in the lab by mixing 50 g of PEG-20K in 450 mL of LR and then transferring the solution to a sterile Intravia container using a 0.2 μ m MediaKap hollow fiber media filter for filtration sterilization.

Orthogonal Polarization Spectral Imaging

Orthogonal Polarization Spectral Imaging (OPSI) was used as a primary indicator of microcirculatory flow and perfusion in both the LPS and CLP models. OPSI images and video samples were captured and saved to a computer for analysis using a handheld OPSI camera made by CapiScope. Samples were taken in the terminal ileum after an enterotomy was performed and the site thoroughly washed of mucus and feces using warm LR and gentle blotting with wet gauze. Once the area was clear, 5-7 video samples were taken that were approximately 5 seconds in length to ensure 4-5 samples of sufficient quality for analysis. Samples were taken at specific time points, at baseline or before shock (in the LPS model), just prior to or at shock (both models), and 30 & 60 minutes after shock (both models). Videos were analyzed by hand to give a microvascular flow index (MFI) score and a proportion of perfused vessels (PPV%).²² Each video sample was assessed for overall picture quality and those with low quality were discarded; low quality indicated by blurriness, significant camera movement, and video length being less than 5 seconds. Videos that were of sufficient quality were analyzed with a grid overlay with at least three equidistant vertical and horizontal lines (Figure 4.A). MFI was determined by looking

at the four major quadrants made by the grid and determining the predominant flow in each respective quadrant and giving each quadrant a score from 0 to 3 (Figure 4.B). Flow was characterized as absent (0), intermittent (1), sluggish (2), or normal (3). The MFI score was the average of the scores across all four quadrants. To calculate PPV, first the total number of vessels that crossed each of the six equidistant grid lines (3 vertical and 3 horizontal) was counted for each line and then the number of those vessels that had either no flow or intermittent flow was recorded. With the total number of vessels crossing each line and the total number of vessels without or with intermittent flow PPV% for each line could be calculated as follows: $100 \times (\text{total number of vessels} - [\text{no flow} + \text{intermittent flow}]) / \text{total number of vessels}$.²³⁻²⁵ The average of all gridlines is taken as the overall PPV% for that video sample.

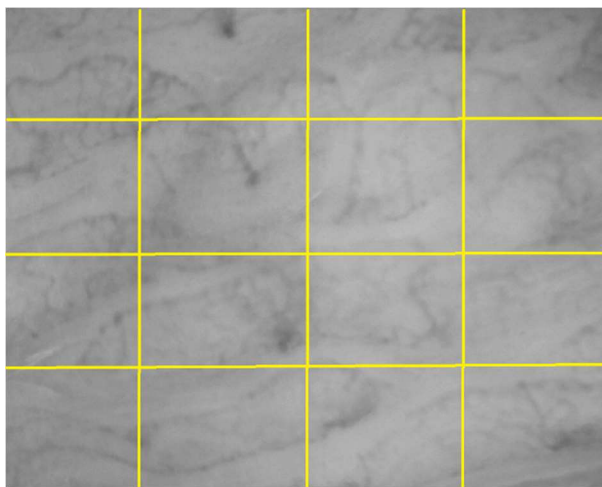


Figure 4.A. Still photo of an OPSI video (Normal flow) - A still photo of a baseline OPSI video with normal perfusion throughout. Larger vessels, 100 μm or wider, are mostly venules and smaller vessels are mostly capillaries. A grid overlay is used while analyzing video samples to calculate vessel density, where the number of vessels crossing the lines is divided by the total length of the lines. From here, the perfusion is graded as either intermittent, no flow, or normal flow. Proportion of perfused vessels (PPV%) is calculated from these values.²³

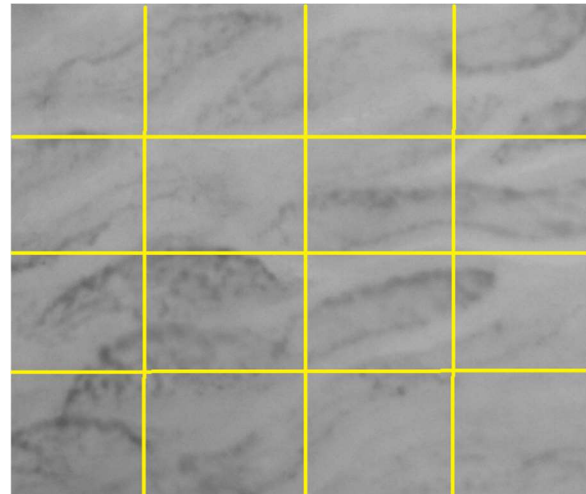


Figure 4.B. Still photo of an OPSI video (Poor flow) - A still photo of a OPSI video taken at shock with absent or intermittent flow throughout. The 16 quadrants above are further divided into 4 even quadrants and classified as one of four flow types, based on the overall flow of each quadrant. Absent or no flow = 0, intermittent flow = 1, sluggish flow = 2, and normal flow = 3. Overall MFI score for each video sample is the average score for all four quadrants.²³

Syndecan-1 ELISA

Syndecan-1 (rat specific) was assayed in rat serum samples from the LPS study using an ELISA assay (Ray Biotech, Peachtree Corners, GA) according to the manual. Briefly, serum samples were diluted 1:1 with assay diluent and 100 µl of diluted sample was added to sample wells of a 96 well plate containing a syndecan-1 specific capture antibody bound to the bottom of the wells. Authentic syndecan-1 standards were used to form a standard curve with each 96 well plate. After the samples and standards equilibrated at 4 C for 18 hours, the unbound syndecan was washed and a secondary syndecan-1 detection antibody linked to horseradish peroxidase was added to the wells. After 90 minutes at room temperature, the unbound detection antibody was washed away, and a substrate was added to each well. Color development from the HRP reaction was stopped at 20 minutes by adding an acetic acid solution. The amount of color development was determined by measuring the wells for absorbance at 405 nm using a Biotech Synergy plate reader. Unknown amounts of syndecan-1 in the samples was extrapolated from a standard curve comparing color development with known amounts of syndecan-1 standard. The results were corrected for dilution and expressed as ng/ml serum. Samples on the low end of the curve were reported as the lowest standard value and samples exceeding the upper limits were diluted and re-assayed until they fell within the linear portion of the standard curve. Each sample was assayed in triplicate and the values were averaged after any outliers were removed (values outside of 10% of the average of the closest 2).

Statistical Analysis

All data was tested for distribution normality. Most of the data were analyzed by parametric one-way ANOVA with Tukey's HSD multiple comparison correction. A Kaplan-Meier survival curve was created to compare LR and PEG survival and Log-rank test. Arterial

blood gas lab values were analyzed with t-tests to compare the PEG group to the LR group. Most data were expressed as the mean plus or minus the standard deviation. Statistical analysis was performed using Microsoft Excel and Prism GraphPad software. Statistical significance was considered a P value of less than 0.05.

Troubleshooting

Due to the nature of working with live animals and surgical procedures that needed to be learned and mastered, a fair number of challenges were overcome along the course of each study. In the LPS model, there was an inconsistency in the potency of LPS between bottles of LPS. Whenever a new bottle needed to be ordered, the largest available bottle was ordered, and the lot/batch number was kept the same when possible. Despite ordering from the same lot, inconsistencies remained and were remedied with an increase in LPS dose to get the desired shock effect within a similar time frame and infusion volume as for other rats, altering the dose from 5 mg/kg all the way to 15 mg/kg when appropriate.

Initial LPS OPSI analysis was done by a single individual in a non-blinded manner. In order to correct for this oversight, approximately 20% of total LPS OPSI video samples were selected at random by another member of the lab, blinded, and reanalyzed by the same individual and then compared against the original analysis. One group of video samples from each treatment group and each time point was selected at random for this blind analysis. When compared to the original analysis there was no significant difference in results. Subsequent CLP OPSI analysis was performed by multiple members of the lab to ensure consistency.

RESULTS

OPSI Analysis

All rats used in the LPS model showed significantly decreased perfusion in their terminal ileum at the point of shock when compared to their own baseline (Figure 5). Rats who were treated with PEG-20K LVR showed significant improvement in perfusion with significant increases in MFI and PPV% at the 30-minute post-shock time point (Figure 5). There was a significant difference between treatment groups at the 30-minute point for both MFI and PPV% (Figure 5) as well as a significant difference in PPV% at the 60-minute point (Figure 5.B). LPS OPSI videos were initially analyzed by a non-blinded single person; to correct for this several months after initial analysis one group of video samples was selected from each treatment group at each time point (approximately 20% of the total video samples) and randomized by another member of the lab and reanalyzed and then compared to the original analysis. Comparison between blind and non-blinded analysis revealed no significant difference (Table 1).

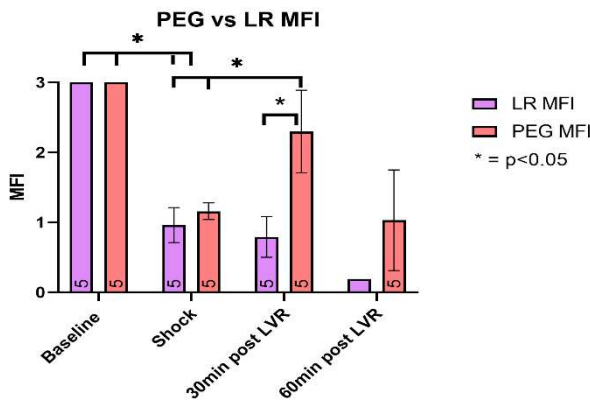


Figure 5.A. Average LPS rat MFI scores - Taken in the terminal ileum using orthogonal polarization spectral imaging (OPSI) throughout LPS infusion. MFI is scored (Y axis) from 0 to 3 and averaged over four quadrants in a video sample, with 0 being no flow, 1 intermittent, 2 sluggish, and 3 normal flow, samples taken at specific time points throughout (X axis). All data are expressed as sample mean +/- standard deviation. P value significance is set at less than 0.05 and is indicated with an asterisk. N for each group is shown at the bottom of each bar.

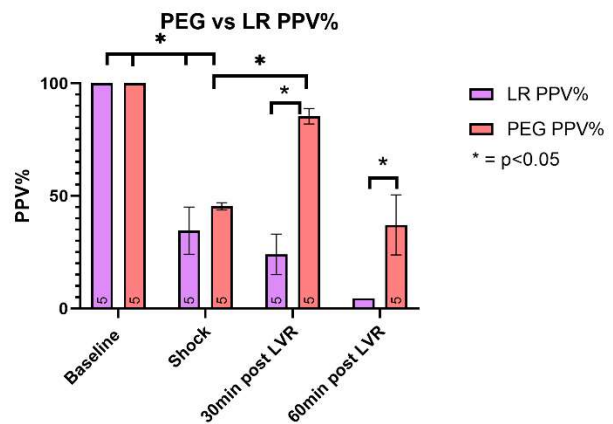


Figure 5.B. Average LPS rat proportion of perfused small vessels (PPV %) - PPV% (Y axis) obtained using OPSI at specific time points throughout LPS infusion (X axis). All data are expressed as sample mean +/- standard deviation. P value significance is set at 0.05 and is indicated with an asterisk. N for each group is shown at the bottom of each bar.

| Timepoint | Blind PEG MFI Mean | Non-Blinded PEG MFI Mean | P Value |
|-----------|--------------------|--------------------------|---------|
| Baseline | 3 ± 0 | 3 ± 0 | P>0.05 |
| Shock | 0.94 ± 0.43 | 1.0 ± 0.50 | P>0.05 |
| 30minutes | 2.85 ± 0.36 | 2.95 ± 0.22 | P>0.05 |
| 60minutes | 0.56 ± 0.50 | 0.56 ± 0.50 | P>0.05 |

| Timepoint | Blind PEG PPV% Mean | Non-Blinded PEG PPV% Mean | P Value |
|-----------|---------------------|---------------------------|---------|
| Baseline | 100 ± 0 | 100 ± 0 | P>0.05 |
| Shock | 43.99 ± 5.65 | 45.27 ± 5.51 | P>0.05 |
| 30minutes | 85.62 ± 3.58 | 85.41 ± 3.97 | P>0.05 |
| 60minutes | 32.54 ± 6.56 | 31.63 ± 6.43 | P>0.05 |

| Timepoint | Blind LR MFI Mean | Non-Blinded LR MFI Mean | P Value |
|-----------|-------------------|-------------------------|---------|
| Baseline | 3 ± 0 | 3 ± 0 | P>0.05 |
| Shock | 0.80 ± 0.40 | 0.70 ± 0.46 | P>0.05 |
| 30minutes | 0.63 ± 0.48 | 0.69 ± 0.58 | P>0.05 |
| 60minutes | 0.19 ± 0.39 | 0.19 ± 0.39 | P>0.05 |

| Timepoint | Blind LR PPV% Mean | Non-Blinded LR PPV% Mean | P Value |
|-----------|--------------------|--------------------------|---------|
| Baseline | 100 ± 0 | 100 ± 0 | P>0.05 |
| Shock | 29.75 ± 8.34 | 23.75 ± 7.82 | P>0.05 |
| 30minutes | 29.11 ± 7.11 | 28.81 ± 6.51 | P>0.05 |
| 60minutes | 8.07 ± 2.23 | 4.52 ± 1.20 | P>0.05 |

Table 1. Blinded Analysis – Blinded analysis data was compared to original non-blinded analysis. All data are expressed as sample mean +/- standard deviation. No significant statistical difference was noted between the comparisons of the two groups.

In CLP rats, baseline terminal ileum samples on Day 1 were not taken due to the invasive nature of the enterotomy needed to obtain OPSI. Additionally, baseline perfusion in all LPS rats was perfect across the board as demonstrated by perfect MFI scores and PPV% (Figure 5). Thus, it was assumed that it was safe to say that the baseline perfusion of the CLP rats would show what we had already seen consistently in all the LPS rats, since they all were treated identically

at baseline. Both treatment groups after shock, but before resuscitation (treatment), saw markedly poor overall perfusion and proportion of perfused small vessels as shown by low MFI scores and PPV% in both groups with an average of 1.07 and 24.9% for LR and 1.12 and 29.0% for PEG (Figure 6). As in the LPS model, PEG-20K treatment groups showed significant perfusion improvement with increased MFI and PPV% from 1.12 and 29.0% to 2.51 and 76.0% (Figure 6). All CLP OPSI video analysis was done individually by several members within the lab and compared for consistency.

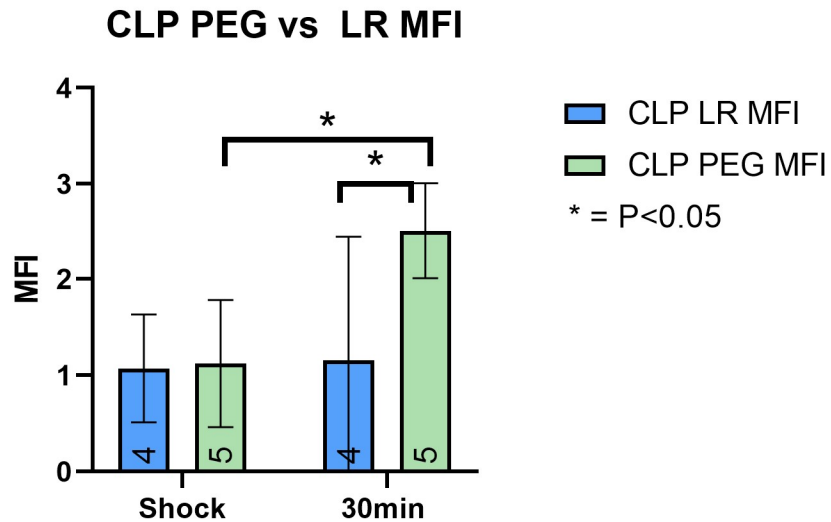


Figure 6.A. Average CLP rat MFI scores - MFI (Y axis) taken in the terminal ileum using OPSI taken just prior to LVR (Shock) and 30 minutes after LVR (30min). All data are expressed as sample mean +/- standard deviation. P value significance is set at less than 0.05 and is indicated with an asterisk. PEG-20K demonstrate significant improvement of overall perfusion after treatment. N for each group is shown at the bottom of each bar.

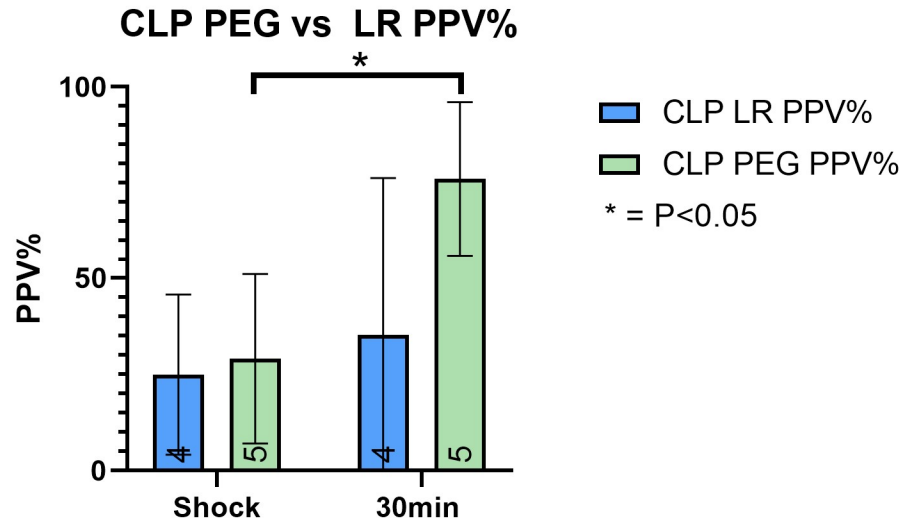


Figure 6.B. Average CLP rat PPV% - PPV% (Y axis) taken in the terminal ileum using OPSI at different time points (X axis) during CLP Day 2. PPV% calculated in the same fashion as LPS model. All data are expressed as sample mean +/- standard deviation. P value significance is set at 0.05 and is indicated with an asterisk. PEG-20K demonstrated a significant improvement in perfusion at the 30-minute post LVR mark while the LR group showed no significant improvement. N for each group is shown at the bottom of each bar.

Lab Values

In the LPS rats all animals had comparable baseline lactate and glucose levels prior to any infusion of LPS with p values all greater than 0.05 when compared (Table 2). Additionally, statistical significance was shown in an increase in lactate for both groups at the point of shock before LVR (Table 3). There was no significant improvement for either group at the 30-minute post-treatment mark; however, there was a significant decrease in lactate in the PEG group at 60-minute post-treatment (Figure 9). Glucose for both groups dropped significantly from baseline to shock and both groups continued to show a steady decline after LVR and through the end of the experiment (Figure 10).

| | LR (n=5) | PEG (n=5) | |
|---------------------------|--------------|--------------|--------|
| Weight | 369.8 ± 30.6 | 346.8 ± 75.5 | p>0.05 |
| Baseline Lactate (mmol/L) | 2.2 ± 0.8 | 3.0 ± 0.7 | p>0.05 |
| Baseline Glucose (mg/dL) | 290.4 ± 50.6 | 259.2 ± 30.9 | p>0.05 |
| Baseline MAP (mmHg) | 92.2 ± 4.4 | 91.4 ± 6.9 | p>0.05 |
| Baseline HR (bpm) | 309.2 ± 37.1 | 307.2 ± 10.4 | p>0.05 |

Table 2. Baseline LPS - This table shows the baseline characteristics of the intervention groups were comparable, with p values greater than 0.05, for LPS rats. All data are expressed as sample mean +/- standard deviation.

| | LR (n=5) | PEG (n=5) | |
|------------------------|--------------|--------------|--------|
| Shock Lactate (mmol/L) | 4.7 ± 0.3 | 6.2 ± 0.2 | p<0.05 |
| Shock Glucose (mg/dL) | 56.4 ± 29.7 | 72.0 ± 47.6 | p>0.05 |
| Shock MAP (mmHg) | 64.6 ± 3.4 | 65.6 ± 3.6 | p>0.05 |
| Shock HR (bpm) | 427.2 ± 14.8 | 420.0 ± 30.6 | p>0.05 |

Table 3. Shock LPS - This table shows the characteristics of the intervention groups at the point of shock (~75% of baseline MAP), prior to administration of low volume resuscitation in LPS rats. All data are expressed as sample mean +/- standard deviation. All values were comparable aside from lactates, where there was statistical significance with the PEG group on average having a higher

LPS PEG vs LR Lactate

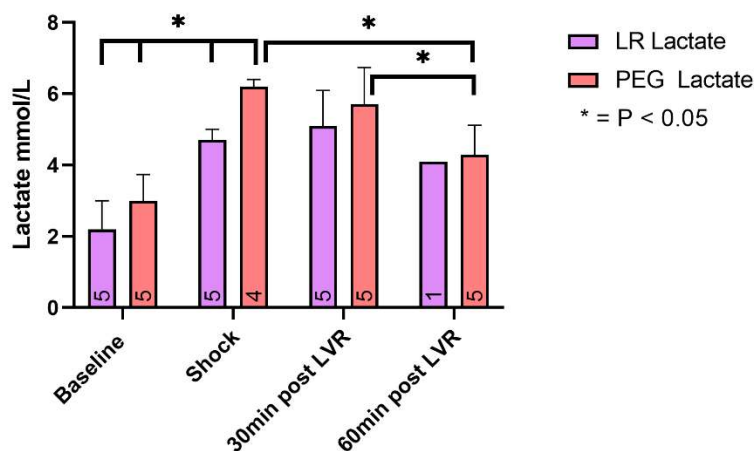


Figure 7. LPS Lactate - Average rat lactate in mmol/L (Y axis) was measured at specific time points (X axis) throughout LPS experiment. Lactate values were obtained from arterial blood gas samples. All data are expressed as sample mean +/- standard deviation. P value significance is set at 0.05 and is indicated with an asterisk. N for each group is shown at the bottom of each bar. A significant increase in lactate from baseline to shock was seen in both groups and a significant decrease was seen in the PEG-20K group at the 60-minute post-treatment mark.

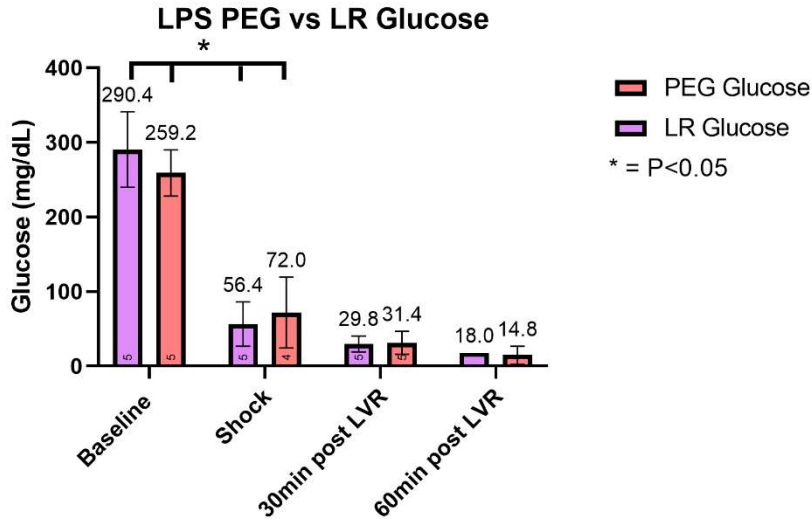


Figure 8. LPS Glucose - Average rat glucose in mg/dL (Y axis) was measured at specific time points (X axis) during LPS. All data are expressed as sample mean +/- standard deviation. Values above error bars are average values. Glucose values were obtained from arterial blood gas samples. P value significance is set at 0.05 and is indicated with an asterisk. N for each group is shown at the bottom of each bar.

In the CLP rats there were significant differences in shock lactate and glucose levels between groups, prior to LVR. Rats that received PEG-20K had a significantly higher lactate and lower glucose, 6.32 versus 2.95 and 87.0 versus 141.5 (Table 4). Despite starting with a higher lactate, the PEG-20K group did not show a significant increase after treatment 6.32 to 7.86, where the LR group showed over a 3x increase from 2.95 to 9.4 (Figure 9). There was a significant decrease in glucose in the LR group after treatment 141.5 to 48.5 and only a minor decrease in the PEG-20K group, 87.0 to 64.6 (Figure 10). Of note, due to errors with the ABG machine, two samples in the 30-minute group of LR were unable to be measured and dropped the n from 4 to 2.

| | LR (n=4) | PEG (n=5) | [†] , n=3; ^{**} , n=4 |
|------------------------|---------------|--------------|---|
| Shock Lactate (mmol/L) | 2.95 ± 1.08 | 6.32 ± 2.05 | p<0.05 |
| Shock Glucose (mg/dL) | 141.5 ± 21.83 | 87.0 ± 33.53 | p<0.05 |
| Shock MAP (mmHg) | 104.4 ± 2.9 | 93.0 ± 15.7 | p>0.05 |
| Shock HR (bpm) | 414.0 ± 38.0 | 437.0 ± 35.0 | p>0.05 |

Table 4. CLP Shock - This table shows that pre-LVR hemodynamics between intervention groups were comparable, with p values greater than 0.05, for CLP rats. All data are expressed as sample mean +/- standard deviation.

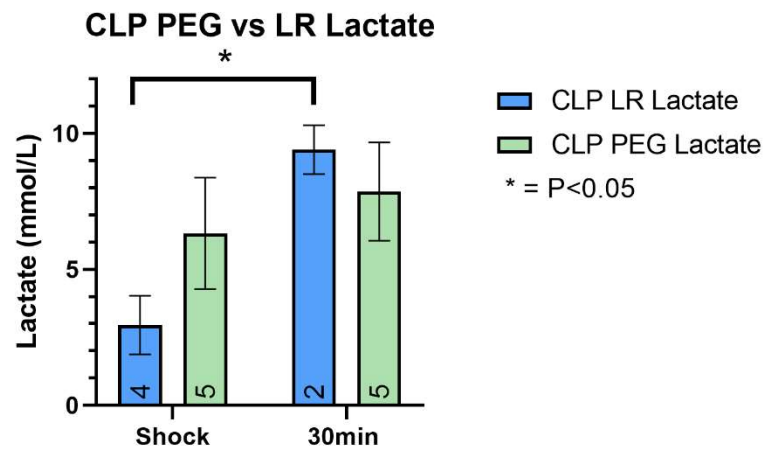


Figure 9. CLP Lactate - Average rat lactate in mmol/L is shown on the Y axis and two time points, just prior to LVR (Shock) and 30 minutes after LVR (30 min) along the X axis. Lactate values were obtained from arterial blood gas samples. All data are expressed as sample mean +/- standard deviation. P value significance is set at 0.05 and is indicated with an asterisk.

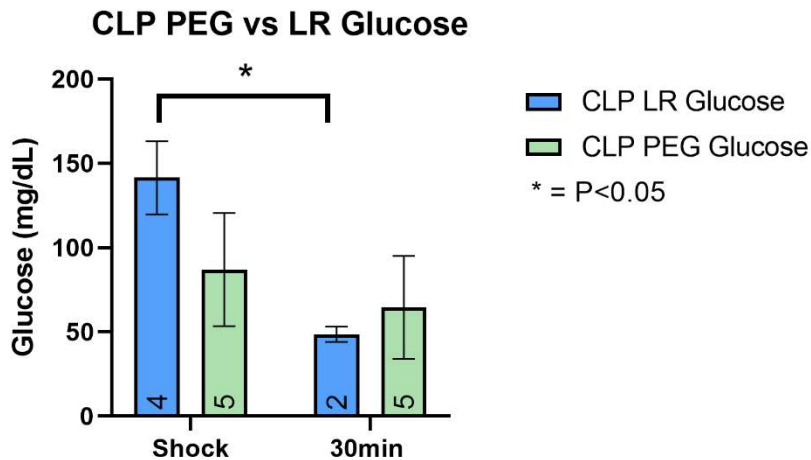


Figure 10. CLP Glucose - Average rat glucose in mg/dL (Y axis) was measured at specific time points (X axis) during CLP Day 2. Glucose values were obtained from arterial blood gas samples. All data are expressed as sample mean +/- standard deviation. P value significance is set at 0.05 and is indicated with an asterisk. N for each group is shown at the bottom of each bar. Of note, due to an ABG machine error, two samples from the LR 30-minute time point group were unable to be measured, dropping the n in this time point from 4 to 2.

Vital Signs and Survival Time

In the LPS model all rats showed similar baseline hemodynamic characteristics with p values above 0.05 when comparing the two treatment groups (Table 2). Additionally, the hemodynamic characteristics of both groups at shock were similar (Table 3). Neither group showed significant improvement or decline in either MAP or HR; however, the PEG-20K MAP did improve slightly from 65.6 to 75.6 with a significant difference between treatment groups (Figure 11.A) and HR decreased on average from 420 to 395.4 while the LR MAP continued to decline, and HR continued to climb (Figure 11).

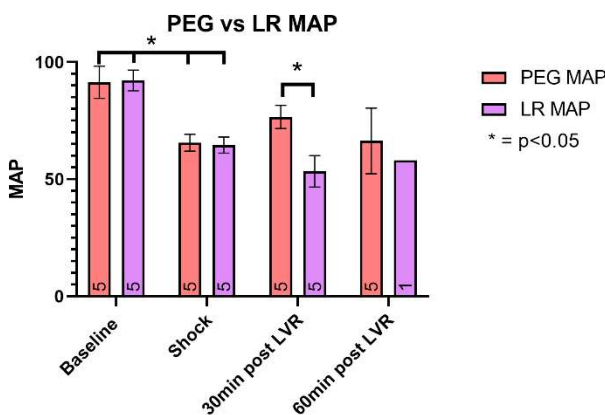


Figure 11.A. LPS MAP - Average MAP (Y axis) is shown at specific timepoints (X axis) throughout the LPS infusion, LVR being low volume resuscitation. All data are expressed as sample mean +/- standard deviation. P value significance is set at less than 0.05 and is indicated with an asterisk. N for each group is shown at the bottom of each bar.

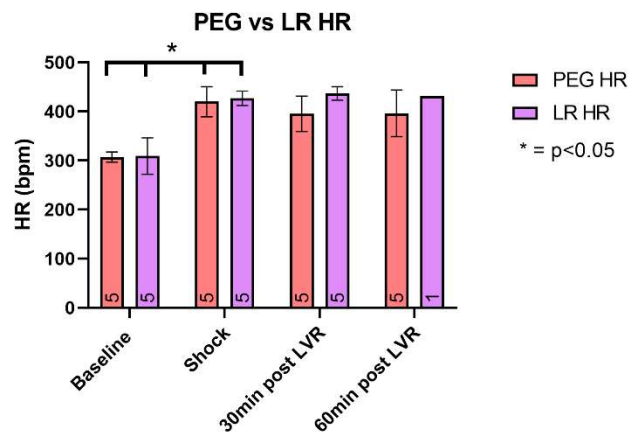


Figure 11.B. LPS HR - Average heart rate on the Y axis is measured in beats per minute and the average is taken at different time points labeled on the X axis, LVR being low volume resuscitation. All data are expressed as sample mean +/- standard deviation. P value significance is set at less than 0.05 and is indicated with an asterisk. N for each group is shown at the bottom of each bar.

In the CLP model as in the LPS model all rats showed similar hemodynamic characteristics just prior to LVR administration (Table 4). Both groups showed a decrease in MAP and HR with a significant decrease in MAP for the PEG-20K group (Figure 12).

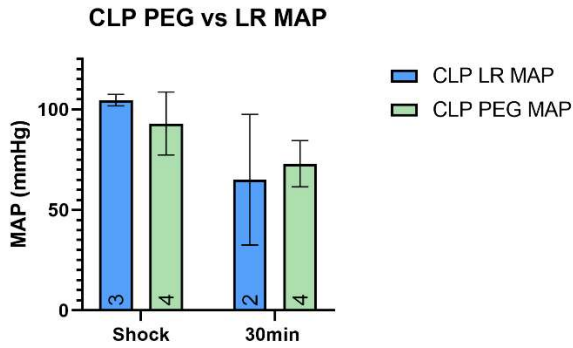


Figure 12.A. CLP MAP - Average rat mean arterial pressure (MAP) in mmHg (Y axis). The two treatment groups LR and PEG-20K are shown. All data are expressed as sample mean +/- standard deviation. N for each group is shown at the bottom of each bar.

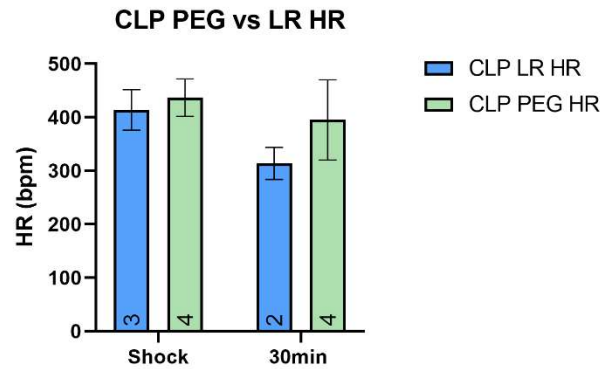


Figure 12.B. CLP HR - Heart rate on the Y axis is measured in beats per minute and the average is taken just prior to LVR (Shock) and 30 minutes after LVR (30min) on the X axis. All data are expressed as sample mean +/- standard deviation. N for each group is shown at the bottom of each bar.

A significant difference was shown between the survival curves of PEG-20K and LR groups in the LPS model. Both groups having an n of 5 to start with, only one rat in the LR group made it past the 60-minute mark with the longest surviving 80 minutes. Every rat in the PEG-20K group made it beyond the 60-minute mark with the longest surviving 195 minutes (Figure 13).

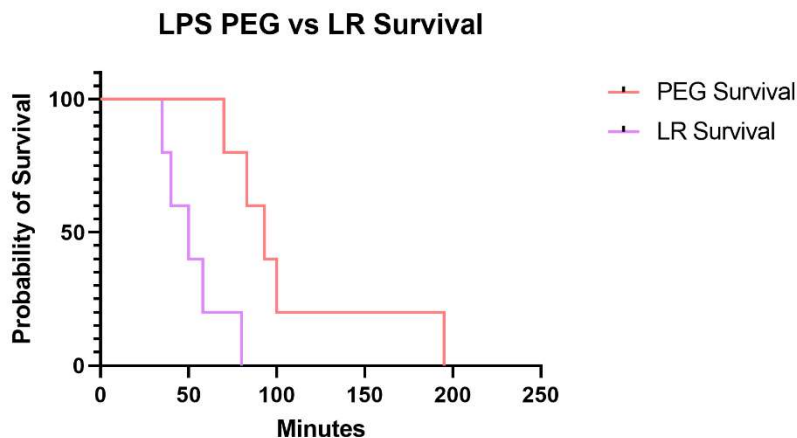


Figure 13. LPS Survival - Kaplan-Meier survival estimate of PEG and LR groups in LPS rats. Measured is the percentage of rats in each respective treatment group (Y axis) alive over time in minutes (X axis). Log-rank (Mantel-Cox) test showed a significant difference in the PEG and LR survival curves.

Syndecan-1 Assay

A Sandwich ELISA was performed to test for the presence of Syndecan-1 in baseline and terminal serum samples collected in the LPS model. Rapid degradation of the core glyocalyx via LPS induced septic shock was shown in both treatment groups. With a P value significance set at 0.05, there was a significant increase in both groups as well as comparable starting levels of Syndecan-1 (Figure 14). There was no significance in Syndecan-1 levels between the two treatment groups.

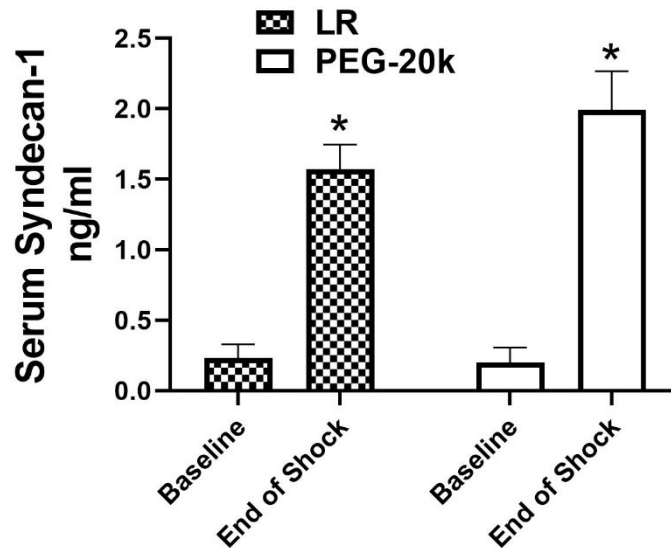


Figure 14. LPS Syndecan-1 - Serum Syndecan-1 was assayed using a Sandwich ELISA. Serum samples were collected at baseline, prior to LPS infusion, and terminal samples just prior to sacrificing the rat after LVR treatment. All data are expressed as sample mean +/- standard deviation. P value significance is set at 0.05 and is indicated with an asterisk. LPS infusion model increased Syndecan-1 shedding in both groups.

DISCUSSION

Major Findings

Sepsis is a serious and life-threatening condition caused by a dysregulated and uncontrolled immune response. If left unchecked, it can progress to septic shock, MODS, and death. Due to the high mortality rates of sepsis and even higher mortality rates of septic shock and the enormous cost in the treatment, for years scientists and clinicians have worked to understand the pathophysiology and develop more meaningful interventions in its treatment. Despite considerable progress, mortality rates remain unacceptably high and measures outside of supportive care are limited. Metabolic cell and tissue swelling in sepsis leads to hypoperfusion of tissues and organs, cascading into further hypoxia and organ failure. Previously in our lab, PEG-20K was identified as an important tool to help improve perfusion in critically ill swine models suffering from metabolic cell and tissue swelling during hemorrhagic shock.^{2,16,17} Since PEG-20K was shown to improve outcomes in models of hypovolemic shock, the next step was to understand the role of metabolic cell and tissue swelling on the microcirculation in septic shock and determine whether PEG-20K could similarly improve outcomes in this setting.

The focus of this research is on the effects of septic shock on the microcirculation in the small intestine and to see if PEG-20K could act as a tool to improve any malperfusion. As such, two different models were used to successfully induce septic shock in rats to compare the cell impermeant intervention to the volume control to test the metabolic swelling hypothesis. There was a significant decrease in microcirculatory perfusion in the small intestine from baseline to shock, as well as significant improvement 30-minutes post LVR with PEG-20K, relative to the LR volume control. No improvement was seen in any rat treated with LR. This trend shows a strong correlation between administration of PEG-20K and improvement of microcirculatory

perfusion, which supports our hypothesis about metabolic cell and tissue swelling involvement in the mechanisms of sepsis-induced changes in tissue perfusion. Additionally, both groups saw a significant increase in blood lactate from baseline to shock with no improvement after LVR in either group. Those rats treated with PEG-20K also saw a significant improvement in survival time when compared to treatment with LR. All of this together makes a strong case for two things: **1.)** Decreased microcirculatory perfusion is significant in septic shock and can be ameliorated with osmotic therapy using hybrid cell impermeants and **2.)** PEG-20K shows promise as a potential therapeutic in clinical septic shock to improve tissue perfusion in the ICU and delay progression of multiple organ failure. More studies need to be done in order to determine how to obtain a more complete picture of the state of the microcirculation in critically ill patients and how PEG-20K may be used as a tool in the clinical setting, but addressing the issue of poor microcirculatory perfusion serves as a promising pathway to improve patient outcomes in the future.

Microcirculatory Changes

The microcirculation of the terminal ileum was observed and measured at different time points throughout each experiment. OPSI was an incredibly difficult skill to master. When being used in a small area of a small animal that is sick and breathing rapidly it makes for a field of view that is constantly moving which makes getting a high-quality video with minimal movement and excellent camera focus difficult. Additionally, if too much pressure was applied, then microvessels would be compressed and provide potentially misleading data. Once mastered though, consistent practice made for excellent quality videos that showed the microcirculation with clarity.

In the LPS model, baseline OPSI recordings were taken prior to the administration of any LPS. Baseline or pre-cecal puncture OPSI was not taken in the CLP model because of the multiple day nature of the experiment. The baseline observations in the LPS model showed excellent perfusion that was consistent and showed no variation and so it was reasonable to expect the same baseline data among the CLP rats. If baselines were taken in the CLP model it would have required a bowel resection after baseline samples were obtained, a difficult procedure and possibly detrimental to the model itself. Additionally, a similar expectation was made with the sham LPS rat, its perfusion looked excellent and consistent throughout and so in an effort to have to sacrifice as few animals as possible, only an LPS sham was performed but these data sets were used for baseline values in both sepsis models. .

For baseline OPSI measurements, each rat showed consistently good flow. No microvessels were seen that had intermittent or no flow, only microvessels with consistently normal flow were seen on OPSI. This observation was confirmed by multiple people trained to analyze OPSI samples within the lab. While it is understood that even under the best conditions, not all capillaries are open and perfused simultaneously within the microcirculation, it is possible this observation is due to the nature of the recording device itself. The OPSI device provides green light that is absorbed by the Hb, which then yields an image of illuminated Hb-carrying structures in negative contrast.²⁶ When flow is so universally good within the capillaries, perhaps an artifact is created from the numerous high flow vessels that masks or makes less-active vessels difficult to see. At the point of septic shock in both models, however, flow was significantly reduced and vessels with no or intermittent flow were easily visualized. This finding would suggest that septic shock has a significant impact on the state of the

microcirculation in the small intestine by causing microcirculatory flow outcomes, as measured by OPSI, to be reduced by 50-75% of baseline.

Finally, significant improvement was seen after LVR treatment with PEG-20K at the 30-minute post-treatment mark. While perfusion did not return to the state it was in at baseline, improvement was so significant it is fair to say that 30-minutes post-LVR with PEG-20K the malperfused state of the small intestine had been reversed. Conversely, after LVR with LR there was no significant improvement in perfusion by using the same volume infusion. It is worth noting that when the PEG-20K groups were observed at the 60-minute post-LVR time-point that there was again a significant decrease in perfusion and a return to the state that was seen at the beginning of shock. Since PEG-20K has been shown to be a relatively inert molecule exerting biophysical effects on water movements based on its differential partitioning in the microcirculation, we can conclude that the increase in capillary perfusion after using PEG-20K in septic rats was caused by the known effects of PEG-20K on unidirectional water transfer out of the extravascular space and into the intravascular space. Other effects are possible but less likely given the relative specific biophysical effects attributable to PEG-20K in shock states.

Lactate, Survival Time, and Vital Signs

Lactate is formed by anaerobic glycolysis, when cellular metabolism occurs without oxygen. Increased serum lactate levels may represent tissue hypoperfusion that is occurring during septic shock, acting as an indicator for the buildup of oxygen debt.²⁷ Arterial blood gas samples measured lactate and found a significant increase in lactate from baseline to shock. Significant improvement in the decrease of lactate levels was seen in the PEG-20K treated groups in the LPS model at the 60-minute point. Given that increased lactate levels are one of

two conditions in which a diagnosis of septic shock can be made in humans,²⁷ this finding helps to build confidence in the septic-shock inducing models used in this study. However, the discordance between lactate levels in sepsis and increased perfusion in PEG-20K-treated rats at the 30-minute post-treatment point is difficult to resolve. Two possible explanations are **1.)** Plasma lactate is often an inconsistent measure of tissue perfusion and lags behind repayment of oxygen debt and **2.)** The optimal dose of PEG-20k is not yet known in septic shock. The idea that lactate lags behind repayment of oxygen debt is supported by previous data from other studies performed in our lab where swine hemorrhagic shock model lactate levels were able to return to normal over the course of several hours after treatment with PEG-20K.¹⁷ We believe that, unlike in hemorrhagic shock where one single dose of PEG-20K sustainably corrects the perfusion problem, in septic shock perfusion defects may be more complicated and require a bolus followed by a lower but continuous infusion of the polymer over time. This has been shown to be necessary when correcting tissue perfusion and fluid movements in a model of distributive shock in dogs caused by massive loss of brain stem activity.²⁸

Kaplan-Meier survival curves were created using survival data obtained in this study and we found a significant difference in the PEG-20K and LR curves. Survival time was recorded as minutes survived after LVR treatment. A significant difference in survival curves was found between the PEG-20K and LR groups. Within the PEG-20K group each rat lived past the 60-minute time point and in the LR group only one had survived past 60-minutes. Previous experiments performed in the lab using the LPS model to examine survival time with additional treatment groups to include LR with norepinephrine (NE) and PEG-20K with NE showed similar survival results with PEG increasing survival rate significantly, increased even further with the addition of norepinephrine. It is worth noting that PEG survival was twice that of NE with LR

and that NE served to enhance PEG survival time. These data, when paired with the significant perfusion improvement in the small bowel after PEG-20K, helps bolster the promise of using PEG-20K as a tool to combat metabolic cell and tissue swelling and improve microcirculatory perfusion and patient outcomes. We believe that the increase in tissue perfusion in the polymer-resuscitated group causally explains the increase in survival in that group. In patients, this may translate into longer survival by increasing tissue perfusion in vital organs and delaying the onset and magnitude of multiple organ failure, thereby giving more time and opportunity for antibiotic and surgical source control.

Vital signs were able to demonstrate an interesting story in the lack of significant improvement from vital signs in shock after treatment with PEG, despite improvement in the microhemodynamics. In the LPS model, both groups saw a significant decrease in MAP and increase in HR at the point of shock. Additionally, neither MAP nor HR showed any significant improvement after either treatment group, even within the PEG-20K treatment group where a significant improvement of microcirculatory perfusion was observed. Similarly, within the CLP model there were no significant improvements in MAP or HR after treatment from either group. The average MAP actually showed a further significant decrease after treatment with PEG despite significant microcirculatory improvement. When coupled with the improved survival rates in the LPS PEG group, this information suggests that microhemodynamics is a better indicator of overall status and stability and that improvement in condition may not always be reflected in the macrodynamics. This further emphasizes the idea that having a complete picture of the state of the microcirculation in real time would be helpful in early identification of a patient's worsening condition and the efficacy of treatments in progress. It would be worth further investigation to see if this improvement in perfusion despite no improvement in

macrodyamics is seen in other vital organs like the kidneys and brain, since observation of the microcirculation was limited to the bowel in this study.

Presence of Sydecan-1

Serum samples were collected in the LPS model prior to LPS infusion and just prior to euthanasia of the animal and the end of the experiment. The presence of Syndecan-1 within the serum indicates a rapid degradation of the core glycocalyx with LPS and this degradation was shown in both the PEG-20K and LR groups. This also is a strong indicator that PEG-20K does not prevent this degradation of the glycocalyx. Due to the limitations of the time points studied and because the two groups had differences in survival and end of study times, it is not possible to make a statement either way about the involvement of the glycocalyx in septic shock outcomes. Syndecan-1 would need to be measured at a common time in both groups after LPS to obtain a clearer understanding of what role PEG-20K may play in the **rate** of degradation of the glycocalyx and not just the absolute amount.

Limitations and Future Studies

There were several limitations having to do with the skills required to perform the experimental models. First, each model involved specific animal surgical skills that required a significant amount of practice with relatively steep learning curves in the case of no prior experience in this area. Everything from delicate dissection down to and around arteries and veins to be cannulated to gentle mobilization, removal, and cleaning of the bowel required experience that could only be obtained through doing. Collection of data samples also presented challenges, obtaining quality OPSI samples was a skill on its own and maintaining patency of

tiny arterial and venous lines throughout long experiments required specific troubleshooting knowledge.

The experimental models themselves proved to be difficult to consistently get to work. Different stock bottles of LPS had varying levels of potency which led to some experiments needing significant increases in doses and a fair amount of trial and error in getting the dose down for each individual bottle of LPS that was used. For the CLP model, there is a significant amount of variability inherent to the experimental design itself that is incredibly difficult to control. Specifically, while each rat shared similar characteristics like sex, weight, and age, their cecum varied greatly in stool amount and consistency which would mean that, despite consistent ligation placement and punctures, there would be differences in stool leakage rates and amounts. In addition to this each rat surely had varying gut microbiotas that may have made the condition of some rats more or less severe.

OPSI measurements as they are done now, even with proper training, can be subjective and differ based on the individual doing the analysis, since every part of the analysis is done by hand. The best way to combat this is through randomization and comparing analysis among several different individuals, which were both done in this study. Everything from how much pressure was used when capturing the video to the monitor used to analyze them can allow for variation in quality of the data obtained. A computer program that would be able to consistently identify, properly grade, and analyze the OPSI videos directly would help to maintain consistency. If such a program were able to do this analysis in real time it would be hugely beneficial in the clinical setting to get an idea of the microcirculatory state in real time.

Finally, the inert polymers used in this study to alter water transfer out of tissues improves perfusion but does not kill bacteria so this will not fix the infection that caused sepsis. This is not

a limitation of the study per se but a limitation of the treatment effect in translational studies. However, inasmuch as PEG-20K increases capillary perfusion in tissues, it may aid in the distribution of antibiotics to sequestered tissues not previously well-perfused and aid in antibiotic effectiveness.

Proposed future experiments would use models for septic shock that can more reliably induce septic shock within a consistent time frame at a consistent severity. Our lab plans to create a more consistent peritoneal sepsis model by placing plates with *Escherichia coli* on them in the abdomen of rats for a more consistent and predictable progression into septic shock. Another area for future work would involve the improvement in and development of technology that can consistently give meaningful values for microcirculatory flow in real time. OPSI is an incredible tool, but its invasive nature and incredible amount of time that goes into analysis by hand makes its clinical applicability severely limited. Inducing sepsis and septic shock in animal models is incredibly difficult to do at a consistent severity. Even in humans, the development, severity, and progression of sepsis and septic shock varies greatly by individual. Any experiment that would be able to reliably induce sepsis at a consistent severity would help overcome the limitations mentioned and continue down the path to improving clinical interventions and patient outcomes.

CONCLUSION

In conclusion, the purpose of this study was to understand the effects of septic shock on the microcirculation of the small intestine and determine whether PEG-20K could be used as a tool to alleviate the observed perfusion deficiencies. Two models were used to successfully induce septic shock, LPS and CLP, and the effects of shock on the microcirculation and subsequent LVR treatments with PEG-20K and LR were measured and analyzed using OPSI. Lactate and other blood chemistry values were obtained using arterial and venous blood samples. Survival time in the LPS model was measured and compared between treatment groups. A clear and significant decrease in microcirculatory perfusion during septic shock was shown using OPSI when compared to baseline samples. Significant improvement in perfusion was shown in both models 30 minutes after LVR treatment with PEG-20K and no improvement was seen when using only LR. This improvement in perfusion had a positive impact on the survival outcomes for the rats treated with PEG-20K when compared with those treated with LR. Lactate levels significantly increased from baseline in both groups, indicating a build-up of oxygen debt and repayment of that debt started to show at the 60-minute point with a significant decrease in lactate from values obtained at shock. This improvement is slower than the improvement seen in perfusion but is demonstrating similar results seen in previous studies in the Mangino lab where lactate levels were able to eventually return to baseline, but this turn around was at a much slower and steadier pace.¹⁷ If a less severe model of septic shock were used and the rats were able to live longer it is possible that we would see the lactate continue to decrease over the course of several hours. The models used in this study were so severe that the animals were unable to live long enough to repay the oxygen debt that was built up in septic shock.

Further studies will allow for clarification on how PEG-20K IV solution can be further used as a tool to improve patient outcomes by dosing studies. The septic shock experimental models aimed to understand the state of the microcirculation during critical illness and to explore a potential tool to intervene at a root level of the problem. Intervening at the source of the problem, lack of perfusion secondary to metabolic cell and tissue swelling, has the potential to vastly improve patient outcomes and decrease mortality rates for sepsis and septic shock in the future.

REFERENCES

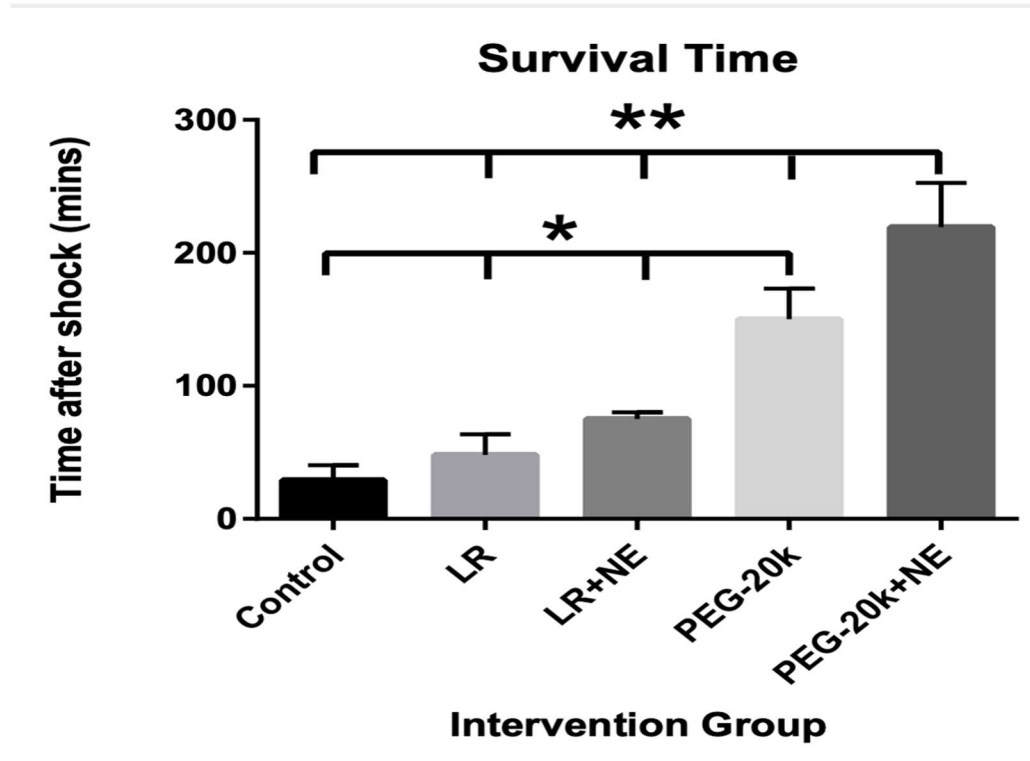
1. Hotchkiss RS, Moldawer LL, Opal SM, Reinhart K, Turnbull IR, Vincent JL. Sepsis and septic shock. *Nat Rev Dis Primers*. 2016;2. doi:10.1038/nrdp.2016.45
2. Parrish D, Lindell SL, Reichstetter H, Aboutanos M, Mangino MJ. Cell impermeant-based low-volume resuscitation in hemorrhagic shock : a biological basis for injury involving cell swelling. *Ann Surg*. 2016;263(3):565-572. doi:10.1097/SLA.0000000000001049
3. Majno G. The Ancient Riddle of Sepsis. *J Infect Dis*. 1991;(May):1-15.
4. Bone RC, Sibbald WJ, Sprung CL. The ACCP-SCCM consensus conference on sepsis and organ failure. *Chest*. 1992;101(6):1481-1483. doi:10.1378/chest.101.6.1481
5. Gyawali B, Ramakrishna K, Dhamoon AS. Sepsis: The evolution in definition, pathophysiology, and management. *SAGE Open Med*. 2019;7:205031211983504. doi:10.1177/2050312119835043
6. Kaukonen KM, Bailey M, Suzuki S, Pilcher D, Bellomo R. Mortality related to severe sepsis and septic shock among critically ill patients in Australia and New Zealand, 2000-2012. *JAMA*. 2014;311(13):1308-1316. doi:10.1001/jama.2014.2637
7. Guven G, Hilty MP, Ince C. Microcirculation: Physiology, Pathophysiology, and Clinical Application. *Blood Purif*. 2020;49(1-2):143-150. doi:10.1159/000503775
8. Dunn JOC, Mythen MG, Grocott MP. Physiology of oxygen transport. *BJA Educ*. 2016;16(10):341-348. doi:10.1093/bjaed/mkw012
9. Pontiga F, Gaytán SP. An experimental approach to the fundamental principles of hemodynamics. *American Journal of Physiology - Advances in Physiology Education*. 2005;29(3):165-171. doi:10.1152/advan.00009.2005
10. Krogh A. The number and distribution of capillaries in muscles with calculations of the oxygen pressure head necessary for supplying the tissue. *J Physiol*. 1919;52(6):409-415. doi:10.1113/jphysiol.1919.sp001839
11. De Backer D, Creteur J, Preiser JC, Dubois MJ, Vincent JL. Microvascular blood flow is altered in patients with sepsis. *Am J Respir Crit Care Med*. 2002;166(1):98-104. doi:10.1164/rccm.200109-016OC
12. Yamamoto Y, Harashima A, Saito H, et al. Septic Shock Is Associated with Receptor for Advanced Glycation End Products Ligation of LPS. *The Journal of Immunology*. 2011;186(5):3248-3257. doi:10.4049/jimmunol.1002253
13. Haussner F, Chakraborty S, Halbgebauer R, Huber-Lang M. Challenge to the intestinal mucosa during sepsis. *Front Immunol*. 2019;10(APR). doi:10.3389/fimmu.2019.00891
14. Kühn F, Schiergens TS, Klar E. Acute Mesenteric Ischemia. *Visc Med*. 2020;36(4):256-263. doi:10.1159/000508739

15. Morelli A, Passariello M. Hemodynamic coherence in sepsis. *Best Pract Res Clin Anaesthesiol.* 2016;30(4):453-463. doi:10.1016/j.bpa.2016.10.009
16. Plant V, Limkemann A, Liebrecht L, et al. Low-volume resuscitation using polyethylene glycol-20k in a preclinical porcine model of hemorrhagic shock. *Journal of Trauma and Acute Care Surgery.* 2016;81(6):1056-1061. doi:10.1097/TA.0000000000001155
17. Khoraki J, Wickramaratne N, Kang HS, et al. Superior Survival Outcomes of a Polyethylene Glycol-20k Based Resuscitation Solution in a Preclinical Porcine Model of Lethal Hemorrhagic Shock. *Ann Surg.* 2022;275(5):E716-E724. doi:10.1097/SLA.0000000000004070
18. Uchimido R, Schmidt EP, Shapiro NI. The Glycocalyx: A Novel Diagnostic and Therapeutic Target in Sepsis. *Crit Care.* Published online 2019:1-12.
19. Becker BF, Jacob M, Leipert S, Salmon AHJ, Chappell D. Degradation of the endothelial glycocalyx in clinical settings: Searching for the sheddases. *Br J Clin Pharmacol.* 2015;80(3):389-402. doi:10.1111/bcp.12629
20. Patterson EK, Cepinskas G, Fraser DD. Endothelial Glycocalyx Degradation in Critical Illness and Injury. *Front Med (Lausanne).* 2022;9(July):1-13. doi:10.3389/fmed.2022.898592
21. Boettcher M, Esser M, Trah J, et al. Markers of neutrophil activation and extracellular traps formation are predictive of appendicitis in mice and humans: a pilot study. *Sci Rep.* 2020;10(1):1-7. doi:10.1038/s41598-020-74370-9
22. Boerma EC, Mathura KR, van der Voort PHJ, Spronk PE, Ince C. Quantifying bedside-derived imaging of microcirculatory abnormalities in septic patients: a prospective validation study. *Crit Care.* 2005;9(6):601-606. doi:10.1186/cc3809
23. De Backer D, Hollenberg S, Boerma C, et al. How to evaluate the microcirculation: Report of a round table conference. *Crit Care.* 2007;11(5):1-9. doi:10.1186/cc6118
24. Riedijk MA, Milstein DMJ. Imaging sublingual microcirculatory perfusion in pediatric patients receiving procedural sedation with propofol: A pilot study. *Microcirculation.* 2018;25(6):1-7. doi:10.1111/micc.12484
25. Boerma EC, Mathura KR, van der Voort PHJ, Spronk PE, Ince C. Quantifying bedside-derived imaging of microcirculatory abnormalities in septic patients: a prospective validation study. *Crit Care.* 2005;9(6):601-606. doi:10.1186/cc3809
26. Genzel-Boroviczény O, Strötgen J, Harris AG, Messmer K, Christ F. Orthogonal polarization spectral imaging (OPS): A novel method to measure the microcirculation in term and preterm infants transcutaneously. *Pediatr Res.* 2002;51(3):386-391. doi:10.1203/00006450-200203000-00019
27. Lee SM, An WS. New clinical criteria for septic shock: Serum lactate level as new emerging vital sign. *J Thorac Dis.* 2016;8(7):1388-1390. doi:10.21037/JTD.2016.05.55

28. Kang HS, Wickramaratne N, Liebrecht LK, Mangino MJ. Effects of polyethylene glycol-20k IV solution on donor management in a canine model of donor brain death. *Biomedicine and Pharmacotherapy*. 2022;152(June):113293. doi:10.1016/j.biopha.2022.113293

APPENDICES

Previous LPS Experiment Survival Data



Previous LPS Experiment Intervention Group Table

| | INTERVENTION GROUP | | | | | p>0.05 |
|-------------------------------|--------------------|-------------|---------------|-------------|----------------|--------|
| | Control (n=3) | LR (n=3) | LR + NE (n=3) | PEG (n=5) | PEG + NE (n=3) | |
| LPS (MG) | 17.1 ± 9.6 | 15.1 ± 8.3 | 11.5 ± 5.0 | 12.1 ± 3.2 | 9.9 ± 3.2 | p>0.05 |
| LPS (MG)/TIME TO SHOCK (MINS) | 0.05 ± 0.004 | 0.05 ± 0.01 | 0.04 ± 0.03 | 0.04 ± 0.04 | 0.04 ± 0.003 | p>0.05 |
| MAP AT SHOCK (MMHG) | 74.3 ± 5.5 | 75.0 ± 3 | 74.3 ± 2.9 | 74.8 ± 3.3 | 72.3 ± 6.4 | p>0.05 |
| LACTATE AT SHOCK (MMOL/L) | 5.2 ± 0.2 | 5.8 ± 1.9 | 6.8* | 5.8 ± 1.3 | 6.5* | p>0.05 |
| NE (MCG) | 0 | 0 | 113.0 ± 9.1 | 0 | 152.4 ± 119.4 | p>0.05 |

*n=2 and standard deviation/statistical analysis not performed

LPS PEG Acid-Base ABG Lab Values

| pH | | | |
|-----------------|--------|-------|---|
| PEG | Mean | SD | n |
| Baseline | 7.25 | 0.08 | 5 |
| Shock | 7.36 | 0.06 | 4 |
| 30min | 7.32 | 0.04 | 5 |
| 60min | 7.25 | 0.12 | 5 |
| 120min | | | 1 |
| pCO2 (mmHg) | | | |
| PEG | Mean | SD | n |
| Baseline | 49 | 10 | 5 |
| Shock | 31 | 3 | 4 |
| 30min | 40 | 1 | 5 |
| 60min | 50 | 21 | 5 |
| 120min | 50 | 0 | 1 |
| pO2 (mmHg) | | | |
| PEG | Mean | SD | n |
| Baseline | 477.00 | 53.58 | 5 |
| Shock | 440.50 | 62.58 | 4 |
| 30min | 375.60 | 87.18 | 5 |
| 60min | 300.00 | 92.68 | 5 |
| 120min | 462.00 | 0.00 | 1 |
| HCO3 (mEq/L) | | | |
| PEG | Mean | SD | n |
| Baseline | 19.32 | 2.69 | 5 |
| Shock | 18.53 | 1.73 | 4 |
| 30min | 19.98 | 1.86 | 5 |
| 60min | 18.86 | 2.30 | 5 |
| 120min | 22.30 | 0.00 | 1 |

LPS LR Acid-Base ABG Lab Values

| pH | | | |
|-----------------|--------|-------|---|
| PEG | Mean | SD | n |
| Baseline | 7.25 | 0.08 | 5 |
| Shock | 7.36 | 0.06 | 4 |
| 30min | 7.32 | 0.04 | 5 |
| 60min | 7.25 | 0.12 | 5 |
| 120min | | | 1 |
| pCO2 (mmHg) | | | |
| PEG | Mean | SD | n |
| Baseline | 49 | 10 | 5 |
| Shock | 31 | 3 | 4 |
| 30min | 40 | 1 | 5 |
| 60min | 50 | 21 | 5 |
| 120min | 50 | 0 | 1 |
| pO2 (mmHg) | | | |
| PEG | Mean | SD | n |
| Baseline | 477.00 | 53.58 | 5 |
| Shock | 440.50 | 62.58 | 4 |
| 30min | 375.60 | 87.18 | 5 |
| 60min | 300.00 | 92.68 | 5 |
| 120min | 462.00 | 0.00 | 1 |
| HCO3 (mEq/L) | | | |
| PEG | Mean | SD | n |
| Baseline | 19.32 | 2.69 | 5 |
| Shock | 18.53 | 1.73 | 4 |
| 30min | 19.98 | 1.86 | 5 |
| 60min | 18.86 | 2.30 | 5 |
| 120min | 22.30 | 0.00 | 1 |

VITA

Charles Payne was born in Alexandria, VA in 1993 and graduated from John R. Lewis High School in 2011. In 2013 he became an EMT and a paramedic in 2018. He went on to attend Virginia Commonwealth University for his undergraduate career from which he obtained a Bachelor of Science in Biology with a minor in Chemistry in 2020. Since then, he has pursued a Master's in Physiology and Biophysics. He has since been awarded the Charles C. Clayton award by the Virginia Commonwealth University School of Medicine as an outstanding rising second year graduate student, as well as the Poland Award, in honor of Dr. James Poland. He was also nominated for the School of Medicine's Phi Kappa Phi award by the Graduate Program's Leadership Committee. He will begin medical school at Virginia Commonwealth University in the coming fall semester.